Metrol. Meas. Syst., Vol. 30 (2023) No. 4, pp. 839–850
DOI: 10.24425/mms.2023.147948

PAN POLSKA AKADEMIA NAUK

METROLOGY AND MEASUREMENT SYSTEMS
Index 330930, ISSN 0860-8229
www.metrology.wat.edu.pl

M&MS

NON-DESTRUCTIVE DETECTION OF HIGH-STRENGTH WIND TURBINE BOLT LOOSENESS USING DIGITAL IMAGE CORRELATION

Wei-Guo Xie[1)], Peng Zhou[1)], Li-Yun Chen[1)], Guo-Qing Gu[2)], Yong-Qing Wang[3)], Yu-Tao Chen[4)]

1) Yancheng Institute of Supervision & Inspection on Product Quality, Yancheng 224056, China (377259207@qq.com)
2) School of Civil Engineering, Yancheng Institute of Technology, Yancheng 224051, China (✉ gqgu@ycit.edu.cn)
3) School of Electrical Engineering, Yancheng Institute of Technology, Yancheng 224051, China (3129254@qq.com)
4) School of Mechanical Engineering, Yancheng Institute of Technology, Yancheng 224051, China (2602967155@qq.com)

Abstract

Looseness of high-strength wind turbine bolts is one of the main types of mechanical failure that threaten the quality and safety of wind turbines, and how to non-destructively detect bolt loosening is essential to accurate assessment of operational reliability of wind turbine structures. Therefore, to address the issue of looseness detection of high-strength wind turbine bolts, this paper proposes a non-destructive detection method based on *digital image correlation* (DIC). Firstly, the mathematical relationships between the in-plane displacement component of the bolt's nut surface, the bolt's preload force loss and the bolt loosening angle are both deduced theoretically. Then, experimental measurements are respectively conducted with DIC with different small bolt loosening angles. The results show that the bolt loosening angle detection method based on DIC has a detection accuracy of over 95%, and the bolt's preload force loss evaluated by the deduced relationship has a good agreement with the empirical value. Therefore, the proposed DIC-based bolt loosening angle detection method can meet the requirements of engineering inspection, and can achieve quantitative assessment of preload forces loss of wind turbine bolt.

Keywords: Bolt looseness detection, digital image correlation, loosening angle, preload force loss.

1. Introduction

Wind power possesses the advantages of low environmental pollution, fast installation, and low carbon emission, making it a mainstay in the development of the global green new energy industry [1]. However, with the installation of a large number of wind turbines, safety accidents such as broken spindles, falling impellers, broken blades and collapsed towers have occurred frequently, and the quality and safety of wind turbines have received widespread attention. High-strength bolts are used to connect the wind turbine components, mostly the tower, impeller, hub,

Article history: received July 17, 2023; revised August 18, 2023; accepted September 5, 2023; available online November 15, 2023.

gearbox, and other key parts [2], which are subjected to cyclic alternating loads in operation, and the bolts are prone to fatigue and even fracture. Numerous survey reports show that the main cause of wind turbine bolt breakage and dislodgement is the loosening of the bolts [3]. Although many detection techniques and sensors have been developed to be applied to bolt looseness detection, detecting this fault is still an unmet industrial need and no widely recognized means of detection or industry standards have been established. Therefore, accurate detection of wind turbine bolt looseness has become an urgent engineering issue.

Currently, the traditional looseness detection methods for high-strength wind turbine bolts are mainly based on manual on-site inspection methods [4] and contact sensing-based bolt loosening detection methods [5]. The manual on-site inspection methods mainly include hammering, marking, magnetic stripe attachment, torque wrenching, and strain gauge testing, *etc.* Although the manual on-site inspection method is simple, it does not allow for the timely detection of loose bolts, has poor timeliness, and requires intensive training in advance. The detection results generally depend on the experiences and subjective perceptions of the inspector, and there are differences in the results. On the other hand, the contact sensing-based bolt loosening detection methods mainly include ultrasonic [6], piezoelectric impedance [7], magnetic field [8], optical *fiber Bragg grating* (FBG) [9], *etc.* Although these contact sensing-based bolt loosening detection methods have a certain application base and attain productive results in some specific application scenarios, such as steel bridges [10], aircraft skins [11], mechanical equipment [12], and so on, there are also disadvantages such as the high price of testing sensors and equipment, the need for manual assistance in the operation process and the difficulty of replacing the equipment regularly, which make it impossible to apply to long-term, high-volume loosening testing of high-strength wind turbine bolts. Consequently, it is quite necessary to develop non-contact, low-cost, efficient, and intelligent methods for wind turbine bolt loosening detection.

To this end, machine vision-based image recognition technology is emerging in the field to meet the increasingly requirements for non-destructive detection. Preliminary researches on machine vision-based image recognition of bolt loosening detection method have also been studied. For example, Park *et al.* proposed a vision-based bolt loosening detection technique for a wind turbine tower [13]. In this method, a combination of the Hough transforms and the Canny edge detection algorithm allows the bolt loosening angle to be deduced by tracking the rotational trajectory of the bolt boundary. Nguyen *et al.* presented a vision-based detection algorithm for the loosening monitoring of steel tube connection nodes in *wind turbine tower* (WTT) structures [14]. Subsequently, Cha *et al.* put forward an improved bolt loosening detection method based on a combination of an image processing algorithm and *support vector machines* (SVM) to identify bolt loosening angle [15]. Recently, both Huynh *et al.* [16] and Yang *et al.* [17] have proposed a vision-based image recognition of bolt loosening smart detection method through a combination of image recognition algorithm and a deep learning recognition algorithm. The above-mentioned methods have indeed gained a good effect in bolt loosening detection, however, they exhibit not only a poor detection of small loosening angles of bolts, but also a high volume of operations and processor requirement.

In order to address the problem of the accurate detection of small loosening angles of bolts, a non-destructive detection method of high-strength wind turbine bolt looseness based on *digital image correlation* (DIC) is innovatively proposed in this paper. Due to its advantages of non-contact, full-field, high-precision measurement of deformations and strains, DIC has been widely used in the fields of material testing, experimental mechanics, aerospace, automotive engineering, and so on [18–20]. As it is well known, a DIC calculation algorithm is carried out based on the grey value matching of the specimen surface's speckle patterns before and after deformation, which essentially belongs to an image recognition algorithm. Specifically, DIC obtains whole-

Metrol. Meas. Syst., Vol. 30 (2023), No. 4, pp. 839–850
DOI: 10.24425/mms.2023.147948

field deformation and strain distribution by correlating the reference subset in the reference speckle pattern with the target subset in the deformed speckle pattern [21, 22]. To the best of our knowledge, there are rare studies on the use of DIC in looseness detection of high-strength wind turbine bolts. In this paper, the principle of using DIC in bolt looseness detection is first investigated theoretically, deducing the mathematic relationship between the loosening angle and the in-plane displacement. Then, a DIC detection experimental setup is established to measure loosening wind turbine bolt surface deformation. Finally, through the loosening angle obtained through DIC calculation, the preload force loss of the loosening bolts is also assessed quantitively.

Results presented in this paper are obtained with MATLAB.

2. Theoretical Analysis

2.1. Brief Synopsis of Digital Image Correlation

At first, we briefly introduce the principle of the DIC method. It employs digital image processing to resolve displacement and deformation gradient fields. The basic principle of the standard subset based DIC is shown in Fig. 1, which is to match the same physical points imaged in the reference image and the deformed image. Towards this, a square subset of $N \times N$ pixels (or the so-called regions of interest) surrounding the tested physical point in the initial image is selected and used to find its corresponding location in the deformed image by defining the maximum value of the calculated correlation coefficient. The vector between the reference subset centre and the target subset centre is the in-plane displacement vector at the interested point $P(x, y)$.

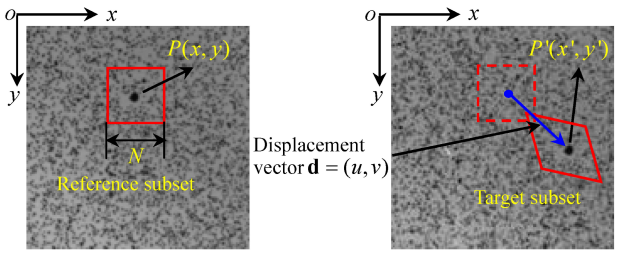

Fig. 1. Schematic for DIC measurement principle.

A correlation coefficient distribution is acquired by moving the reference subset through the searching subset continuously and calculating the correlation coefficient at each location. In practical situations, the ZNCC criterion [23], which is insensitive to the offset and linear change of illumination lighting, is defined below as

$$C(u.v) = \frac{\sum_{i=1}^{n} [f(x_i, y_i) - f_m] \times [g(x_i', y_i') - g_m]}{\sqrt{\sum_{i=1}^{n} [f(x_i, y_i) - f_m]^2} \cdot \sqrt{\sum_{i=1}^{n} [g(x_i', y_i') - g_m]^2}}, \tag{1}$$

where $f(x_i, y_i)$ and $g(x_i', y_i')$ are the intensity values at $(x_i,\ y_i)$ in the reference subset and (x_i', y_i') in the target subset, respectively; u, v are the displacements in the x and y directions, respectively, and $u = x_i' - x_i$, $v = y_i' - y_i$; f_m and g_m are the mean intensity values of the reference and target subset; n denotes the number of pixels contained in the reference subset.

2.2. Calculation of the Bolt Loosening Angle

In this section, the mathematical relationship between the bolt loosening angle and the in-plane displacement is deduced theoretically. As illustrated in Fig. 2, a Cartesian coordinate system is firstly established with the bolt rotation centre O as the original point. $P(x, y)$ denotes the location of an arbitrary corner point of the bolt, and α represents the angle between OP and the x-axis. When the bolt rotates counter clockwise with a small loosening angle φ with respect to the original point, the location of the corner point $P(x, y)$ will then change to $P'(x+u, y+v)$, and the in-plane x and y displacement components u and v of the bolt's corner point $P(x, y)$ can be expressed as

$$u = -PP' \sin\alpha \approx -(OP \cdot \varphi)\sin\alpha = -(OP \cdot \sin\alpha)\varphi = -\varphi y, \tag{2}$$

$$v = PP' \cos\alpha \approx (OP \cdot \varphi)\cos\alpha = (OP \cdot \cos\alpha)\varphi = \varphi x. \tag{3}$$

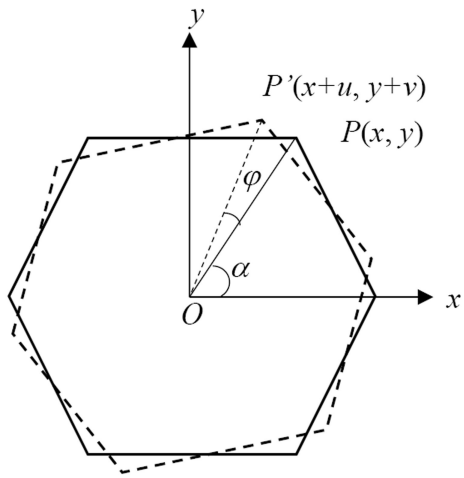

Fig. 2. Schematic for detection of corner points during bolt rotation.

It can be obviously found from (2) and (3) that all the displacement components u and v depend only on the corner point's coordinates y and x, respectively. That is to say, when the displacement components u and v are measured, the rotation angle φ, *i.e.*, the bolt loosening angle, can be obtained resultantly. Therefore, the rotation angle of bolt can be further calculated as

$$\varphi = -\frac{\mathrm{d}u}{\mathrm{d}y}, \quad \text{or} \quad \varphi = \frac{\mathrm{d}v}{\mathrm{d}x}. \tag{4}$$

It is notable that DIC can be utilized for measurement of the displacement components u and v. In fact, only one of the in-plane displacement components is needed for calculation of bolt loosening angle. Owing to DIC's high-precision measurement of displacements, a small loosening angle of bolt can be thus detected by this method.

2.3. Determination of the Preload Force Loss

The process of tightening a bolt may seem simple, but it is in fact a very complex one. The relative rotation of the threads causes the bolt to be progressively elongated and the connected parts to be progressively flattened, with the two parts being firmly joined as a single unit. As the

angle of rotation of the threads increases, the elongation of the bolt, the axial force of the bolt, the equivalent stress of the bolt and the tightening torque of the bolt also increase. In contrast, with the looseness of the bolt, the bolt preload force loss will increase gradually. This section mainly focuses on the quantitative relationship between the bolt preload force loss and the bolt loosening angle.

As it is well known, with torque-controlled bolt tightening, the bolt shaft force is controlled below the yield load (usually taken to be 70% to 90% of the yield load), and the bolt is under the linear elastic phase. The quantitative relationship between the bolt preload force loss and the bolt loosening angle under the linear phase can be expressed as [24]

$$F_M = \frac{P}{360 \cdot (\delta_S + \delta_P)} \cdot \varphi, \tag{5}$$

where P is the pitch of thread; φ is the bolt loosening angle; δ_S and δ_P are the flexibility of the bolt and the clamped part, respectively. Obviously, the linear relationship between the bolt preload force loss and the bolt loosening angle can be easily obtained.

By substituting (4) into (5), the quantitative relationship between the bolt preload force loss and the bolt loosening angle can be also written as

$$F_M = \frac{P}{360 \cdot (\delta_S + \delta_P)} \cdot \frac{\mathrm{d}u}{\mathrm{d}y}, \quad \text{or} \quad F_M = \frac{P}{360 \cdot (\delta_S + \delta_P)} \cdot \frac{\mathrm{d}v}{\mathrm{d}x}. \tag{6}$$

According to (5) and (6), the bolt preload force loss can be evaluated quantitatively, taking advantage of the in-plane displacement component u or v obtained by DIC.

3. Experiments and Results

This section presents an experimental investigation conducted on the proposed DIC-based methodology for loosening detection of the high-strength wind turbine bolts. A genuine wind turbine bolt tested in rotation was used to verify the feasibility and effectiveness of the proposed DIC-based method.

3.1. Bolt Specimen and DIC Test Setup

The experimental specimen tested in rotation was an M36# Dacromet wind turbine bolt with hot dip galvanizing. The examined bolt was made of 42CrMo high-strength steel, and had a nominal diameter of 36 mm and a performance level of 10.9. Table 1 lists the detailed geometric parameters of the tested bolt specimen, and Table 2 lists the detailed material properties of the tested bolt specimen.

Table 1. Geometric properties of the tested bolt specimen.

Property	Parameter
Nominal diameter (mm)	36
Length of bolt (mm)	380
Length of screw (mm)	240
Length of thread (mm)	120
Thread pitch (mm)	4

Table 2. Material properties of the tested bolt specimen.

Property	Parameter
Material type	42CrMo
Young's modulus (Pa)	2.12×10^{11}
Poisson's ratio	0.28
Density (kg/m^3)	7850
Performance level	10.9
Tension strength (MPa)	≥ 1040
Yield strength (MPa)	≥ 940
Elongation after fracture (%)	≥ 9
Shrinkage after fracture (%)	≥ 48

The two-dimensional (2D) DIC experimental setup shown in Fig. 3 was developed for bolt loosening detection. The tested bolt, depicted in the upper-right enlarged image of Fig. 3, was connected by a special customized jig fixed on the vibration-isolated optical table. The middle of the jig was machined with a certain depth of threaded hole. Making use of the bolt external thread, the bolt was screwed to the bottom of the threaded hole of the jig so that it did not rotate. The movable spanner clamped the free end of the bolt, and the standard weights to apply a certain amount of torque were hung at the other end of the spanner.

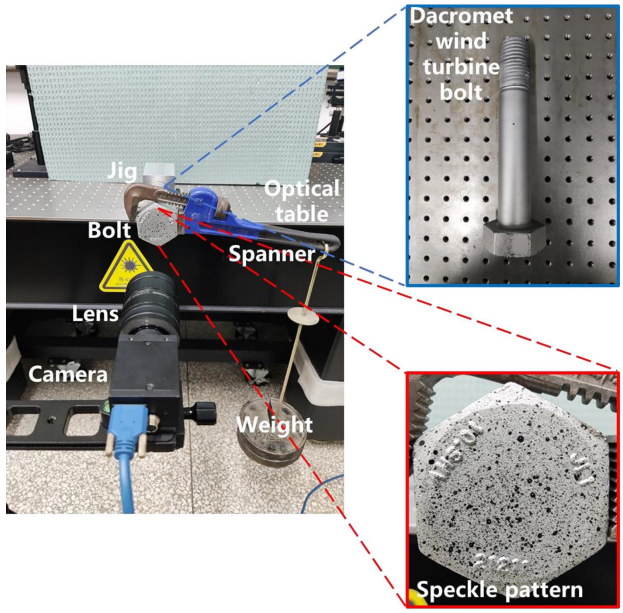

Fig. 3. DIC experimental setup for bolt loosening detection.

Through the rotation of the spanner by addition or subtraction of weights, the bolt looseness scene was simulated. Once bolt looseness occurred due to fatigue, vibration, and so on, the bolt would rotate around its axis, and the surface of the bolt's nut would rotate around the centre of the

nut, and the bolt preload forces would decrease. Therefore, high-precision measurement the nut's rotation angle with the DIC algorithm became an indirect method for non-destructive detection of bolt looseness.

It is well known that the applied speckle pattern on the surface of the bolt specimen plays an important role in the DIC's calculation of accuracy and precision. As illustrated in the bottom-right enlarged image of Fig. 3, a random speckle pattern sprayed on as black matte paint spots was prefabricated on the nut's surface of the tested bolt. In order to capture the speckle patterns before and after the tested bolt specimen rotation, a 5-megapixel (MP) industrial monochrome COMS camera (GS3-U3-51S5M-C, FLIR) with an imaging lens (HF25SA-1, FUJINON) was used for speckle patterns acquisition of the bolt specimen. The camera was mounted on a rigid cross bar fixed on a tripod, levelling the centreline heights of the lens and bolt.

Prior to DIC testing, both the working distance and focal distance of the camera were adjusted such that its *field of view* (FOV) would clearly cover the entire *region of interest* (ROI) of the bolt specimen. The DIC software Ncorr – an open source 2D DIC MATLAB program [25], was used to correlate the recorded speckle images before and after deformation to calculate the full-field displacement distributions on the nut's surface of the tested bolt specimen. According to (4), the rotation angle due to bolt loosening can be determined by one of the in-plane displacement components obtained by the DIC method. Furthermore, the resultant preload force loss can be quantitatively evaluated by means of (6).

3.2. Experimental Results and Discussion

The bolt loosening detection experiments were carried out by counterclockwise rotation of the spanner with different angles. First, the bolt specimen was tightened to the state of ultimate torque by addition of the maximum weights, then counterclockwise rotated to the predetermined angles of 3°, 4° and 5° respectively. It is well known that the torsion angle is proportional to the torque within the elastic range according to the torsion theory of the circular shaft, *i.e.*, $\varphi = Tl/GI_P$, where T denotes the torque, l represents the length, and GI_P means the torsional stiffness. The bolt specimen used herein obviously has an intrinsic l and GI_P. Therefore, the true rotation angle of the bolt can be exactly controlled by proper alteration of the weights exerted to the spanner to change the bolt's torque state. Meanwhile, the camera with a working distance of 300 mm exactly captured the speckle patterns at each state of the bolt specimen. Fig. 4 presents the recorded speckle patterns of the tested bolt specimen' surface at different rotation angles. Setting the 0° speckle pattern as the reference image and the 3°, 4° and 5° speckle patterns as the target images, the Newton-Raphson DIC algorithm was then used to correlate the reference image and target images respectively to calculate the in-plane displacement distributions at each rotation state.

Fig. 5 shows the in-plane displacement components u and v contours on the surface of the tested bolt specimen under 3° loosening angle, which were exactly measured by the DIC method. It is obviously noted from Fig. 5 that the u-field displacement distribution exhibits a linear relationship with regard to the y-coordinate, and the$v$-field displacement distribution exhibits a linear relationship with regard to the x-coordinate as well, which has a good agreement to (2) and (3). Meanwhile, in order to accurately measure the rotation angle, *i.e.*, the loosening angle of the bolt specimen, the data along the vertical and horizontal centrelines of$u$- and v-field displacements distribution were selected and processed respectively.

Figure 6 illustrates the u- and v-field displacement profiles along the vertical and horizontal centrelines AA′ and BB′ on the surface of the bolt specimen, as indicated in the bottom-right and bottom-left corners of the figure. In Fig. 6, the least-squares fit algorithm is, respectively, used to fit the centrelines of raw u- and v-field displacement data obtained by DIC. The fitted linear

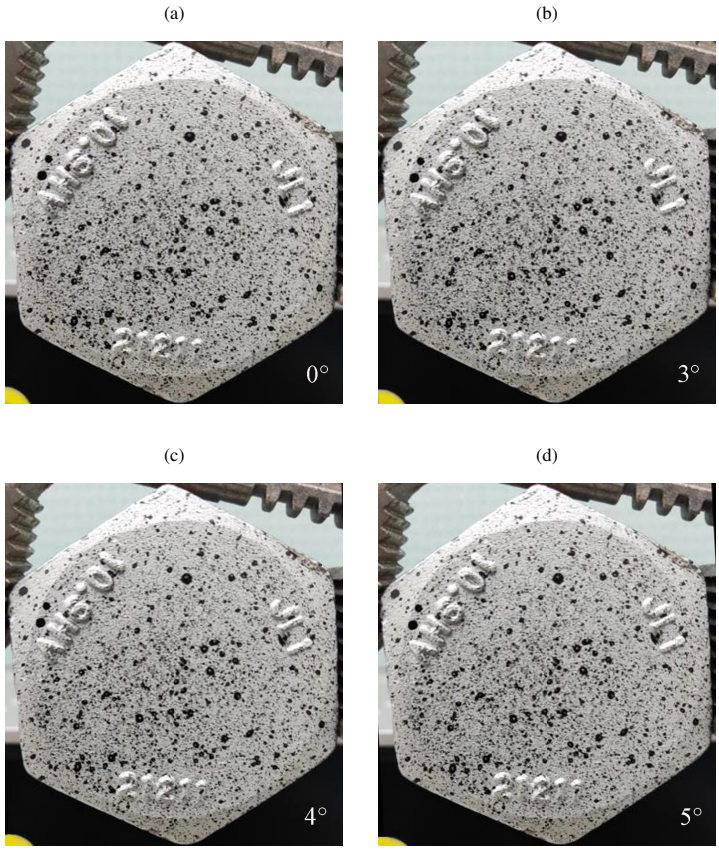

Fig. 4. Recorded speckle patterns with different bolt rotation angles of (a) 0°, (b) 3°, (c) 4°, and (d) 5°.

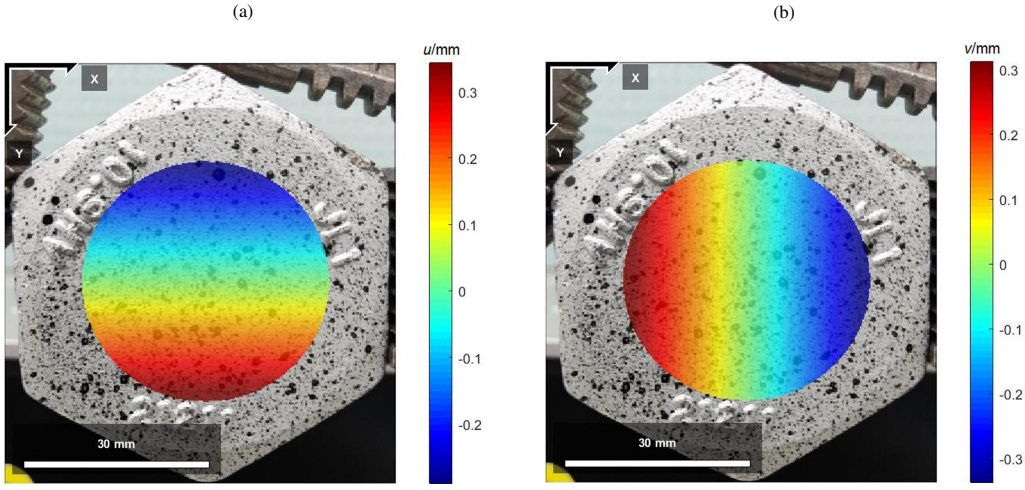

Fig. 5. DIC measured results of the bolt specimen under 3° loosening angle (a) u-field displacement component; (b) v-field displacement component.

functions are $u = 0.05338y - 0.3111$ and $v = -0.05387x + 0.3334$. After angle conversion, the slopes of two linear functions transformed into the angle system are about 3°, and the relative errors are 2.0% and 2.9% respectively, which meets the engineering error requirement very well. It can be obviously found from the experimental results that the proposed DIC-based bolt loosening detection method is truly competent for the practical wind turbine bolt's high-precision testing.

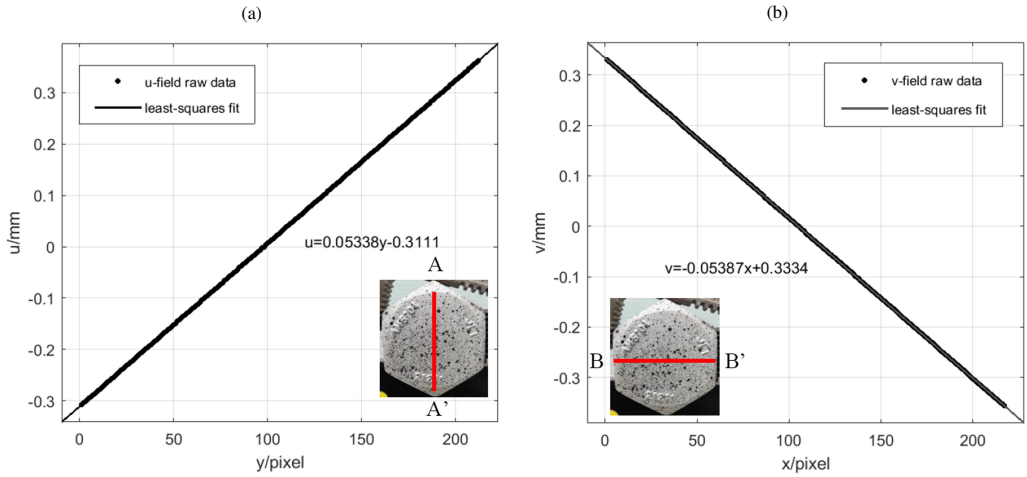

Fig. 6. The in-plane displacement component along (a) vertical centreline AA' and (b) horizontal centreline BB' on the surface of the bolt specimen.

On the other hand, according to (6), the bolt specimen's preload force loss can be obtained with known bolt specimen's thread pitch P and flexibilities of δ_S, δ_P. Here, the bolt specimen's preload force loss under 3° rotation angle is about 24.56 kN. Similarly, the DIC algorithm is subsequently utilized for processing the speckle patterns corresponding to the bolt loosening angles of 4° and 5°. Table 3 shows the experimental results of the detected loosening angle, detection accuracy and preload force loss under different loosening angles. The results from Table 3 indicate that the detected loosening angle obtained by the proposed DIC-based bolt loosening detection method agree with the real loosening angle very well and the detection accuracy can reach more than 95%, which meets the actual wind turbine bolt batch detection requirements. With the increasement of the bolt loosening angle, the accuracy of the proposed DIC-based bolt loosening detection method becomes high accordingly. In addition, for every 1° loosening angle of the M36# bolt, the preload force decreases by an average of 8.2 kN after analysis, which is basically in accordance with the empirical values.

Table 3. Detected results of M36# bolt specimen at different small loosening angles.

Loosening angle (°)	**Detection angle** (°)	**Angle deviation** (°)	**Accuracy** (%)	**Preload force loss** (kN)
3	3.07	0.07	97.7	24.56
4	4.15	0.15	96.2	33.76
5	5.14	0.14	97.2	41.03

4. Conclusions

This paper proposes a non-destructive DIC-based method for detecting the loosening angle of high-strength wind turbine bolt during rotation tests. The presented method allows for the high-precision, noncontact, automated detection of wind turbine bolt's small loosening angle, and also can reach a satisfactory detection accuracy over 95%. Specifically, the detection methodology is based on the fact that the bolt loosening angle is the slope of the linear function between the in-plane displacement component of the bolt surface and the coordinate. It is simplified as a simple rigid body in-plane rotation measurement model and is deduced by the theoretical analysis. Both the feasibility and effectiveness of this methodology are well validated by experiments. Moreover, the preload force loss of the wind turbine bolt under loosening situations is effectively evaluated through using this methodology.

Future studies can focus on the application of this DIC-based methodology to non-destructive on-site detection of wind turbine bolt loosening to provide the quantitative indicators for the detection, for which the online detection of the wind turbine bolt's health condition would present a new challenge. Furthermore, due to the anti-corrosion requirements of actual wind turbine bolts, the traditional contact sensors are difficult for application in the case of long-term, online detection of actual wind turbine bolts. In contrast, the vision-based detection method can become the most promising detection method for *structural health monitoring* (SHM) of wind turbine bolts.

Acknowledgements

This work was supported by the Jiangsu Provincial Market Regulation Administration Science and Technology Project (No. KJ2022049).

References

[1] Lalonde, E. R., Dai, K. S., Lu, W. S., & Bitsuamlak, G. (2019). Wind turbine testing methods and application of hybrid testing: A review. *Wind and Structures*, *29*(3), 195–207. https://doi.org/10.12989/was.2019.29.3.195

[2] Brouwer, S. R., Al-Jibouri, S. H., Cardenas, I. C., & Halman, J. I. (2018). Towards analysing risks to public safety from wind turbines. *Reliability Engineering & System Safety*, 180, 77–87. https://doi.org/10.1016/j.ress.2018.07.010

[3] Rincon-Casado, A., Julia-Lerma, J. M., Garcia-Vallejo, D., & Dominguez, J. (2022). Experimental estimation of the residual fatigue life on in-service wind turbine bolts. *Engineering Failure Analysis*, 141, 106658. https://doi.org/10.1016/j.engfailanal.2022.106658

[4] Li, S. Z., Li, H., Zhou, X. H., Wang, Y. H., Li, X. H., Gao, D., & Zhu, R. H. (2023). Damage detection of flange bolts in wind turbine towers using dynamic strain responses. *Journal of Civil Structural Health Monitoring*, *13*(1), 67–81. https://doi.org/10.1007/s13349-022-00622-z

[5] Civera, M., & Surace, C. (2022). Non-destructive techniques for the condition and structural health monitoring of wind turbines: A literature review of the last 20 years. *Sensors*, *22*(4), 1627. https://doi.org/10.3390/s22041627

[6] Chen, J., He, C. F., Lyu, Y., Zhang, Y., Xie, L. Y., & Wu, L. (2020). Ultrasonic inspection of the surface crack for the main shaft of a wind turbine from the end face. *NDT & E International*, *114*, 102283. https://doi.org/10.1016/j.ndteint.2020.102283

[7] Yue, Y. C., Tian, J. J., Bai, Y. T., Jia, K., He, J., Luo, D., & Chen, T. B. (2021). Applicability analysis of inspection and monitoring technologies in wind turbine towers. *Shock Vibration*, *2021*, 5548727. https://doi.org/10.1155/2021/5548727

[8] Pezzani, C. M., Bossio, J. M., Castellino, A. M., Bossio, G. R., & De Angelo, C. H. (2014). Bearing fault detection in wind turbines with permanent magnet synchronous machines. *IEEE Latin America Transactions*, *12*(7), 1199–1205. https://doi.org/10.1109/TLA.2014.6948853

[9] Sampath, U., Kim, H., Kim, D. G., Kim, Y. C., & Song, M. (2015). In-situ cure monitoring of wind turbine blades by using fiber Bragg grating sensors and Fresnel reflection measurement. *Sensors*, *15*(8), 18229–18238. https://doi.org/10.3390/s150818229

[10] Kim, S. T., Yoon, H., Park, Y. H., Jin, S. S., Shin, S., & Yonn, S. M. (2011). Smart sensing of PSC girders using a PC strand with a built-in optical fiber sensor. *Applied Sciences*, *11*(1), 359. https://doi.org/10.3390/app11010359

[11] Kim, D., Han, S., Kim, T., Kim, C., Lee, D., Kang, D., & Koh, J. S. (2021). Design of a sensitive balloon sensor for safe human-robot interaction. *Sensors*, *21*(6), 2163. https://doi.org/10.3390/s21062163

[12] Chen, C. X., Ma, T. H., Jin, H., Wu, Y. Y., Hou, Z. W., & Li, F. (2020). Torque and rotational speed sensor based on resistance and capacitive grating for rotational shaft of mechanical systems. *Mechanical Systems and Signal Processing*, *142*, 106737. https://doi.org/10.1016/j.ymssp.2020.106737

[13] Park, J. H., Huynh, T. C., Choi, S. H., & Kim, J. T. (2015). Vision-based technique for bolt-loosening detection in wind turbine tower. *Wind and Structures*, *21*(6), 709–726. https://doi.org/10.12989/was.2015.21.6.709

[14] Nguyen, C. U., Lee, S. Y., Huynh, T. C., Kim, H. T., & Kim, J. T. (2019). Vibration characteristics of offshore wind turbine tower with gravity-based foundation under wave excitation. *Smart Structures and Systems*, 23, 405–420. https://doi.org/10.12989/sss.2019.23.5.405

[15] Cha, Y. J., You, K., & Choi, W. (2016). Vision-based detection of loosened bolts using the Hough transform and support vector machines. *Automation in Construction*, *71*, 181–188. https://doi.org/10.1016/j.autcon.2016.06.008

[16] Huynh, T. C. (2021). Vision-based autonomous bolt-looseness detection method for splice connections: Design, lab-scale evaluation, and field application. *Automation in Constructio*, *124*, 103591. https://doi.org/10.1016/j.autcon.2021.103591

[17] Yang, X. Y., Gao, Y. Q., Feng, C., Zhang, Y., & Wang, W. (2022). Deep learning-based bolt loosening detection for wind turbine towers. *Structural Control and Health Monitoring*, *29*(6), e2943. https://doi.org/10.1002/stc.2943

[18] Pan, B., Zhang, X. Y., Lv, Y., L. P., & Yu, T. (2022). Automatic optimal camera exposure time control for digital image correlation. *Measurement Science and Technology*, *33*(10), 105205. https://doi.org/10.1088/1361-6501/ac750e

[19] Han, S. H., He, Y. M., Lei, J., Tian, Y., Hu, Y. Y., Xie, Y. Y., & Yang, Y. B. (2023). Analysis of displacement fields with large deformations using an improved spectral digital image correlation method. *Optik*, *283*, 170901. https://doi.org/10.1016/j.ijleo.2023.170901

[20] Wang, L., Liu, G. Y., Deng, Y. W., Sun, W. Z., Ma, Q. W., & Ma, S. P. (2023). Investigation on out-of-plane displacement measurements of thin films via a mechanical constraint-based 3D-DIC technique. *Optics Communications*, 530, 129015. https://doi.org/10.1016/j.optcom.2022.129015

[21] Gu, G. Q., She, B., Xu, G. Z., & Xu, X. (2017). Non-uniform illumination correction based on the retinex theory in digital image correlation measurement method. *Optica Applicata*, *47*(2), 199-208. https://doi.org/10.5277/oa170203

[22] Su, Y. (2023). An analytical study on the low-pass filtering effect of digital image correlation caused by under-matched shape functions. *Optics and Lasers in Engineering*, *168*, 107679. https://doi.org/10.1016/j.optlaseng.2023.107679

[23] Khoo, S. W., Karuppanan, S., & Tan, C. S. (2016). A review of surface deformation and strain measurement using two-dimensional digital image correlation. *Metrology and Measurement Systems*, *23*(3), 461–480. https://doi.org/10.1515/mms-2016-0028

[24] Kong, Z. Y., Jin, Y., Hong, S. Z., Liu, Q. W., Vu, Q. V., & Kim, S. E. (2022). Degradation behavior of the preload force of high-strength bolts after corrosion. *Buildings*, *12*(12), 2122. https://doi.org/10.3390/buildings12122122

[25] Blaber, J., Adair, B., & Antoniou, A. (2015). Ncorr: Open-Source 2D Digital Image Correlation Matlab Software. *Experimental Mechanics*, *55*(6), 1105–1122. https://doi.org/10.1007/s11340-015-0009-1

Weiguo Xie received the B.Sc. degree from Jiangnan University in 2008. He is currently a Senior Engineer of the Yancheng Institute of Supervision & Inspection on Product Quality. His main research interest is mechanical engineering and mechanical measurement system design.

Liyun Chen received the M.Sc. degree from Nanjing Tech University in 2009. He is currently a Senior Engineer of the Yancheng Institute of Supervision & Inspection on Product Quality. His main research interest is mechanical testing and NDT.

Peng Zhou received the B.Sc. degree from the Yancheng Institute of Technology in 2008. He is currently an Assistant Engineer of Yancheng Institute of Supervision & Inspection on Product Quality. His main research interest is mechanical testing.

Guoqing Gu received the Ph.D. degree from the Nanjing University of Aeronautics & Astronautics in 2013. He is currently an Associate Professor of the School of Civil Engineering of the Yancheng Institute of Technology. His research activity focuses on experimental mechanics.

Yongqing Wang received the Ph.D. degree from the Nanjing University of Science and Technology in 2017. He is currently a lecturer at the Yancheng Institute of Technology. His main research interest is industrial automation testing and photoelectric detection.

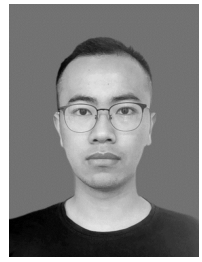

Yutao Chen received the B.Sc. degree from Changshu Institute of Technology in 2022. He is a full-time graduate student at the Yancheng Institute of Technology. He majors in mechanical automation, with main focus on structural health monitoring.